

ULTRASONIC NON-DESTRUCTIVE TESTING: SYSTEM SELECTION FOR CHARACTERISATION AND DETECTION OF DEFECTS IN REPAIRED COMPOSITE MATERIALS

Hannah R. Spratling and Matthew E. Ibrahim

Platforms Division, Defence Science and Technology Group,
506 Lorimer St, Fishermans Bend VIC 3207

Abstract

This paper presents a study of the effect of ultrasonic non-destructive testing system selection on the detection and sizing of defects in repaired polymer-matrix composite materials. We provide a quantitative study of the variance due to ultrasonic test parameters and arrays on the sizing of epoxy-repaired delaminations, and the detection of barely visible impact damage (BVID).

Keywords: ultrasonic testing, composite repair, non-destructive testing

1. General Introduction

Ultrasonic testing detects defects in structural materials via changes in acoustic impedance, which can be related to mechanical stiffness. It is therefore very effective in the testing of composite materials containing internal air-based defects. Ultrasonic testing is capable of providing quantitative measurements of defect location, size and depth, as well as being able to distinguish between delaminations, micro-cracking, voids, inclusions, and porosity [1]. While in-field ultrasonic non-destructive testing (NDT) is conventionally undertaken using contact phased array ultrasonic equipment, immersion ultrasonic testing is useful for characterizing damage in a laboratory setting on manufactured defects to study features such as defect size, growth and depth in advanced aerospace composites. When compared to contact ultrasonics, immersion testing undertaken in a water bath offers superior consistency in acoustic coupling and a reduction in the degree of distortion of the converted electrical-pressure signals [2]. However, due to the requirement of the specimen needing to be submerged in a water tank, this method is less practical. Immersion ultrasonic testing typically involves immersing a test sample in a water bath with the incident piezoelectric transducer arranged at a suitable standoff distance perpendicular to the front surface of the sample. The subsequent reflections are then received by either the same transducer, operating as a synchronized pulse-echo send-receive device, or by a second receiving transducer placed behind the sample and detecting the through-transmitted signal.

Transmission of a sound beam through an immersed test material may be illustrated using a two-interface ray-tracing diagram as shown in Figure 1. This diagram shows the multiple reflections and transmissions that occur at each interface as the energy is propagated within the specimen.

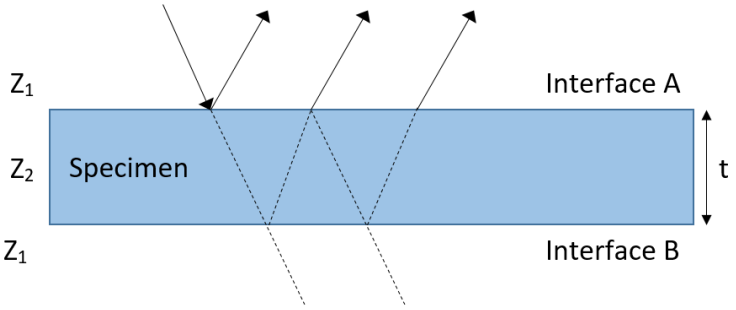


Figure 1 – Ray tracing diagram of a two-interface material system, indicating how an ultrasonic pulse is refracted through the media and reflected off and transmitted across the interfaces.

The system employed to collect ultrasonic data displays the reflections and transmission of sound as a function of time, as a waveform, or 'A-scan', produced by the sound-pressure to voltage piezo-electric conversion, signal amplification and filtering. The resultant pulse-echo and the through-transmission scans show the percentage of sound reflected or transmitted by the material versus the travel time of the sound through the different mediums.

From the A-scan output, the front wall of the material where the sound wave first contacts can be identified from a significant reflection back to the transducer [3]. This 'front-wall echo' (FWE) is the first peak on the output depicted in Figure 2. The successive peaks are echoes from the back wall where the transmitted sound wave travels through the material and continues to reflect back and forth from the front and back walls of the specimen. These 'back-wall echoes' (BWE) continue to reduce in height due to the material attenuation and via the sound that is transmitted out through the back of the specimen into the third medium, water.

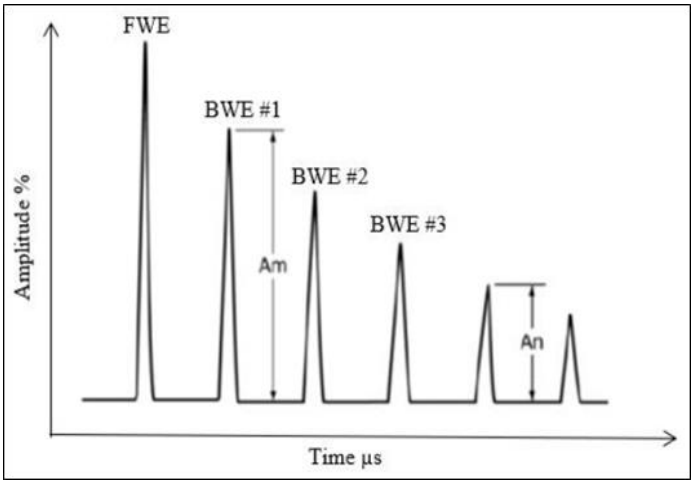


Figure 2 – Pulse- echo A-scan output with labelled echoes, annotated from ASTM E664 [4]. In this case, the waveform has been rectified.

A precision automated pulsed ultrasonic measurement system manufactured by *TecScan Systems Ltd* (Canada) was used to perform immersion scans. The TecScan Scan-3D system consists of a large immersion tank filled with room-temperature water, two 5-degrees of freedom robotic heads which are fitted with suitable ultrasonic immersion transducers, a high signal-to-noise ratio electronic ultrasonic pulsing and data acquisition system, with an integrated software system that performs 3-D scanner head motion control, and data collection and analysis.

The system applies a rapidly pulsed voltage spike or square wave to the transmitting transducer crystal, generating ultrasonic waves according to the piezoelectric effect. The compression waves are subsequently pulsed through the test material at a pulse repetition frequency of up to hundreds of Hertz. The receiving transducer, whether the transmitter or a separate probe, passively acquires

the pressure waves and converts them to electrical signals via the reverse phenomenon.

The positional accuracy of the TecScan Scan-3D system is 0.33 mm in X & Y, 0.83 mm in Z and 0.5° in radial/rotational axes [5]. The gimbal transducer heads (Figure 3) are able to be positioned in 3-D space, their locations stored, and subsequently retrieved to return the system to identical locations between testing events.

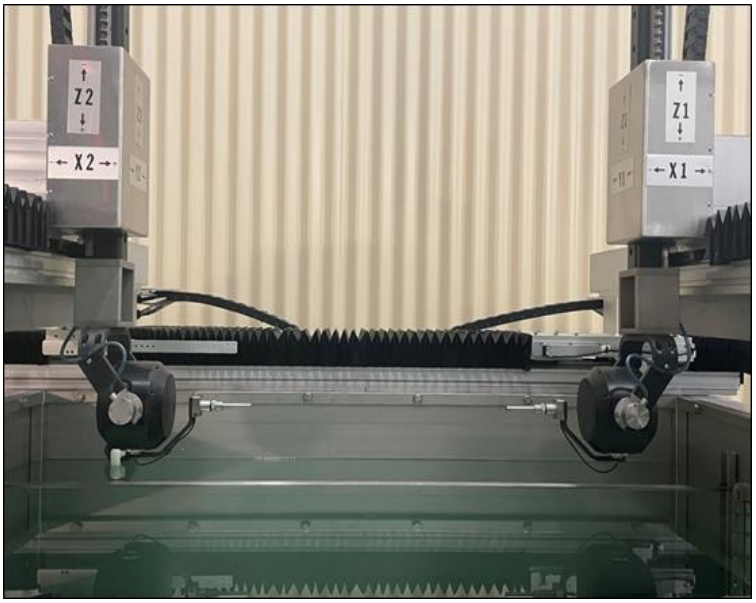


Figure 3 – Photograph of TecScan gimbal heads above the TecScan immersion tank. A pair of acoustically matched 5 MHz pencil immersion probes are fitted to the heads.

The pulse-echo signals obtained from the specimen can be gated (Figure 4) to provide a back-wall echo C-scan; showing the sound reflected from the back interface of the sample, and an internal echo C-scan; showing changes in impedance inside the sample. The through transmission signal indicates the total sound energy transmitted through the specimen and received on the other side. The pulse echo method allows for defect depth analysis, while the through transmission method is most accurate for defect sizing.

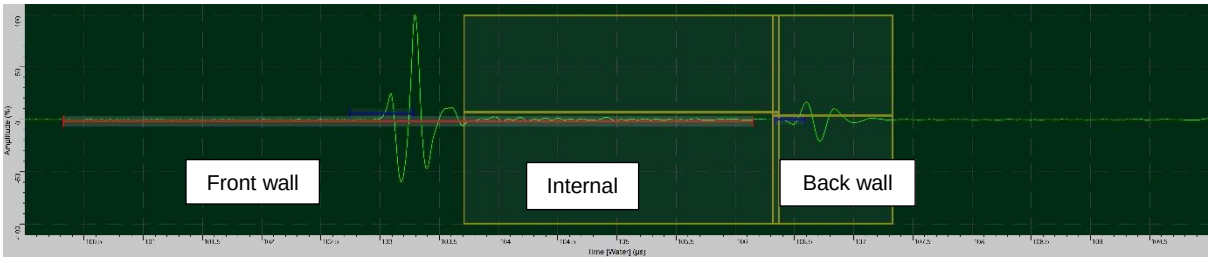


Figure 4 – Pulse echo A-scan of a pristine carbon-polymer composite, with the first peak being the front wall reflection of the specimen and the second peak the back wall reflection. The first yellow box gates the area between the front wall and back wall echoes, measuring any internal reflection due to defects in the material. The second yellow box gates the back wall echo.

When preparing for ultrasonic testing on a new material or system, transducer selection is critical to ensure that any internal defects of interest will be correctly identified. Probe characteristics for single element transducers include nominal frequency, beam size resultant from element diameter and focal length. For each probe, various system parameters were adjusted to ensure that the transducer was not over-powered resulting in an oversaturated signal. These parameters included the input voltage, capacitance and damping.

With increasing ultrasonic frequency the spatial resolution in the thickness direction increases, but is limited by the also increasing frequency-dependent acoustic attenuation of the material [6]. The increasing attenuation reduces the signal clarity of the received reflected and transmitted signals. Spherically concave lenses can be used in immersion NDT to focus the sound to a smaller 'spot size' at the water-to-specimen interface, increasing lateral resolution in a scanning configuration [7]. This beam concentration reduces beam spread and improves beam symmetry, providing more accurate defect sizing. The -6 dB drop method is employed to size defects, and is independent of beam size or diffraction in the beam, but can be influenced by diffraction at the defect edge and asymmetry in the beam [8].

When characterising BVID and internal delaminations in polymer-matrix composites, it can be useful to determine the depth at which the delaminations occur for characterisation and repair purposes. By utilizing the time of flight (TOF) of internal echoes received via pulse-echo, the known speed of sound of the material can be used to determine at what depth these echoes occur within the material. An example of depth analysis on induced delaminations is shown in Figure 5. The depth analysis can in turn be correlated with a specific ply in the material.

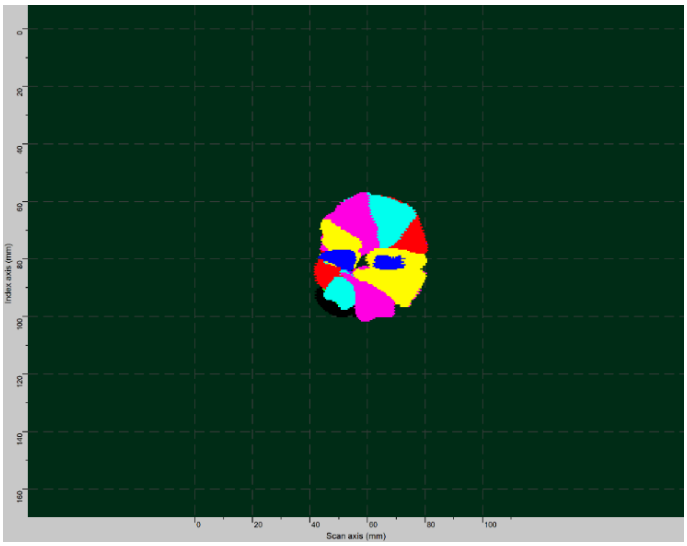


Figure 5 – Depth analysis using TOF of a delamination in a CFRP coupon. Here the defect depth is colour coded.

Acoustic attenuation is an experimentally derived material property that relates to the losses of acoustic energy due to absorption and scattering within the bulk of a material. This is both a frequency- and specimen-specific property dependent on the as-manufactured material [9].

The acoustic attenuation coefficient can be defined in terms of a plane compression wave propagating within the material where the wave amplitude A varies with increasing distance $x > 0$, and time t according to

$$A(x) = A_0 e^{j\omega(t-x/c_p)} e^{-\alpha x} \tag{1}$$

where A_0 is the pressure just inside the front surface of the material, c_p is the sound phase velocity and $\omega = 2\pi f$ is the angular frequency. In ultrasonics, the attenuation coefficient is generally expressed in decibel per centimeter (dB/cm). According to Equation ((2), with this choice of units

$$\alpha\ (\mathrm{dB/cm}) = \frac{20}{x(\mathrm{cm})} \log_{10} \left| \frac{A_0}{A(x)} \right| \tag{2}$$

The acoustic attenuation measurement method used in this paper was proposed by He [9], whereby a combination of the peak amplitude of the frequency content of the front wall echo, back wall echo, signal transmitted through the specimen, and the signal transmitted through the same water path with the specimen removed are employed. Utilising the Fast Fourier Transform (FFT) of the signals reveals

frequency-dependent features that are difficult to identify in the time-domain [10]. The calculation required is presented in Equation (3),

$$\alpha = \frac{1}{T}\left(\ln\left(\frac{A_1}{A_2}\right) - \ln\left(\frac{A_w}{A_s}\right)\right) \times 8.868 \quad (3)$$

where T is the thickness of the specimen in cm, A_1 is the peak amplitude of the specimen front wall echo, A_2 is the amplitude of the first back wall echo, A_w is the peak amplitude of the transmitted signal through water, and A_s is the peak amplitude of the transmitted signal through the specimen. The attenuation is converted from η/cm to dB/cm by multiplying by 8.868.

As the transducers used have finite size, diffraction or beam spreading occurs with increasing axial distance from the transducer face, the Lommel diffraction correction $D(s)$ as implemented by Rogers and Buren [11] to solve the Fresnel diffraction integral, may be used to account for changes in profile of the beam with position.

$$D(s) = \sqrt{\left[\cos\left(\frac{2\pi}{s}\right) - J_0\left(\frac{2\pi}{s}\right)\right]^2 + \left[\sin\left(\frac{2\pi}{s}\right) - J_1\left(\frac{2\pi}{s}\right)\right]^2} \quad (4)$$

where J_0 and J_1 are first order Bessel functions and s is the corresponding Fresnel parameter.

The Lommel-diffraction correction integral accounts for changes in phase and amplitude due to diffraction from the finite-sized transducer beam. The Fresnel parameters used for this particular method are summarised in Equations (5) to (8),

$$s_1 = \frac{2d_1 c_w}{f a^2} \quad (5)$$

$$s_2 = \frac{2d_1 c_w}{f a^2} + \frac{2LV_p(f)}{f a^2} \quad (6)$$

$$s_w = \frac{d c_w}{f a^2} \quad (7)$$

$$s_s = \frac{(d-L) c_w}{f a^2} + \frac{LV_p(f)}{f a^2} \quad (8)$$

where d_1 is the distance between the transducer and the front wall of the specimen, d is the distance between the two transducers, c_w is the speed of sound through water, f is the frequency, a is the radius of the transducer element, L is the thickness of the specimen, and $V_p(f)$ is the sound phase velocity of the specimen. The subscript denotes which amplitude the correction factor should be applied to. S.I. units apply unless specified otherwise.

2. Method

2.1 Transducers

A range of ultrasonic immersion transducer pairs were selected with various combinations of nominal frequency, element diameter and focal length to understand the effect of different system properties on defect sizing. Table 1Table 1 lists the probes used.

Table 1 – Ultrasonic immersion transducers

Nominal frequency (MHz)	Element diameter (inches)	Focal Length (inches)
0.50	1.50	Natural focus
1.00	0.50	Natural focus
2.25	0.50	Natural focus
5.00	0.25	Natural focus
5.00	0.25	3.00
5.00	0.50	1.50
5.00	0.50	3.00
10.00	0.25	1.50
15.00	0.50	3.00

2.2 Test Specimens

This study utilized four 150 mm x 100 mm carbon fibre/epoxy laminate coupons manufactured from Solvay Cycom 7714A/M46J UD carbon-epoxy pre-preg, cured in an autoclave. These 4.5 mm thick panels consist of 32 plies with a stacking sequence of $[+45/0/-45/90]_{4S}$. The samples were impacted in the centre to form internal delaminations with impact energies of 4 J, 6 J, 8 J and 10 J.

A separate repaired carbon-polymer composite panel was inspected to investigate the use of acoustic attenuation as a measurement of repair quality. This panel had a similar layup and a bonded step lap repair. The repair is designed for surface and shallow subsurface damage, including near surface delamination, surface or shallow subsurface fibre-damage, or localized manufacturing defects (e.g. voids, porosity) within the upper plies of a prepreg composite laminate. The damage is removed via ply-by-ply machining to create a stepped cavity, which is then filled with prepreg plies and film adhesive to restore load transfer. The thickness of the pristine, unrepaired section of the panel was 3.6 mm and the repaired section 3.9 mm. A through-transmission C-Scan (Figure 6) of the repaired panel is included to show the repaired section.

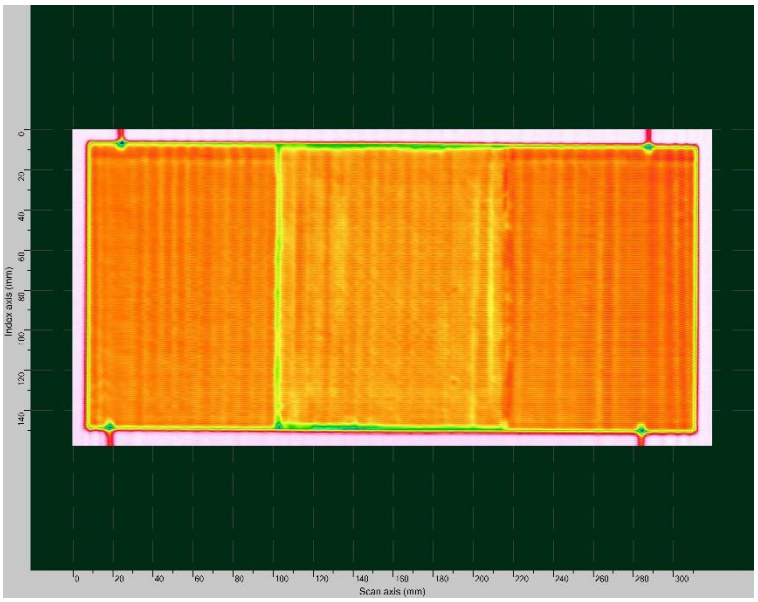


Figure 6 – Through transmission C-Scan of repaired carbon-polymer composite panel. The repair is completed by machining a stepped cavity removing the area of material containing defects, then replacing the material with prepreg plies and adhesive. This area is visible in the centre where it has a slightly higher transmission. A slight shift in the relaying of the plies is visible on the edges of the repair.

2.3 Scan acquisition and analysis

Simultaneous pulse-echo and through-transmission scans were acquired for each of the four coupons, using the nine pre-selected transducer sets, with the pulse probe transmitting at normal incidence to the specimen surface (the medium 1 to medium 2 interface). The pulse-echo scans are

gated to isolate (i) the echo occurring at the rear surface of the specimen, i.e. the BWE, providing the total energy that has not been scattered or absorbed elsewhere within the material thickness, and (ii) an internal pulse-echo scan that provides information on what impedance changes are occurring within the specimen thickness, as well as allowing for time-of-flight (TOF) defect depth analysis. Through-transmission scans provide an averaged measurement of attenuation within the test material by receiving the transmitted signal through the sample, and are used for the most accurate defect sizing and other area measurements. A typical scan set is shown in Figure 7.

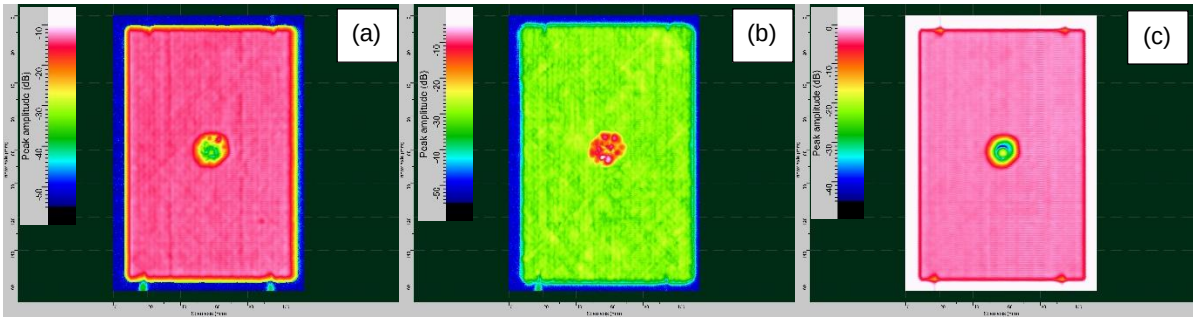


Figure 7 – A typical set of pulse-echo and through transmission scans (using 5 MHz 0.25" element 3" focus). From left to right the scans are; back wall pulse-echo (a), internal pulse-echo (b) and through transmission (c). The impact damage is visible in the centre of each image.

2.4 Sound speed – depth analysis

The sound speed through the material of interest is calculated by using the time between the first back wall echo and the second back wall echo of the ultrasound through the material [12]. The required times may be taken from identical locations on these two echo peaks in the A-scan.

As the elastic properties of a material are temperature dependent, the speed of sound through a medium also depends on its temperature [13]. The speed of sound is related to the stiffness and density of a solid material, Equation (9)

$$v = \sqrt{\frac{M}{\rho}} \tag{9}$$

v is the speed of sound, M is the compression wave modulus of the material, and ρ is the density of the material. The stiffness tensor of carbon-polymer composite materials have a higher complexity compared to isotropic materials, where the ply stacking sequence influences the stiffness of the material.

The speed of sound through the immersion medium is used to determine the distances between the ultrasonic transducers and the specimen front and back walls, to ensure that the specimen is in the far field of the beam for naturally focused transducers, or at the focal distance for focused transducers. As the speed of sound is temperature dependent, for each set of scans, the water temperature is measured to ensure that transmitting transducer is at the correct standoff distance for each measurement. The through transmission receiving transducer is then placed as close as practical to the rear surface of the specimen to ensure all of the sound transmitted at that material interface is captured by the receiving probe.

The speed of sound is also required to use TOF data for defect depth analysis. The measured speed of sound of the impact samples is 2606 m/s, which is in the typical range for aerospace-grade carbon-fibre composite laminates.

2.5 Defect sizing

Defect sizing for damage that has straightforward geometry in the XY plane can be readily achieved using a standard method based on classic beam shadowing [8]. It is assumed (for a defect that is much larger than the ultrasonic beam 'spot size'), that once half of the energy of the beam has been lost from its nominal value, that it is symmetrically straddling the defect edge. This is achieved by measuring the loss of half the A-scan peak height in the frequency domain. However, neglecting non-

linearity, measurements are practically often made using the time-domain signal amplitude. The TecScan TecView 2 software, as with typical ultrasonic immersion acquisition and analysis systems, contains automated software tools to colour-code and determine the area of defect regions. The tool is set by the operator to select all locations within the C-scan, in which the selected peak height is at 50% (-6 dB) or less than the nominal pristine material value, in order to detect the boundaries of, and size, the defect.

Given that pristine areas of a material will exhibit a range of energy transmission values, these can be averaged or specified against the 6 dB drop to determine the most accurate background level, whilst also avoiding any edge-diffracted signals, typically occurring at the specimen's physical edges. An output using this method is shown in Figure 8.

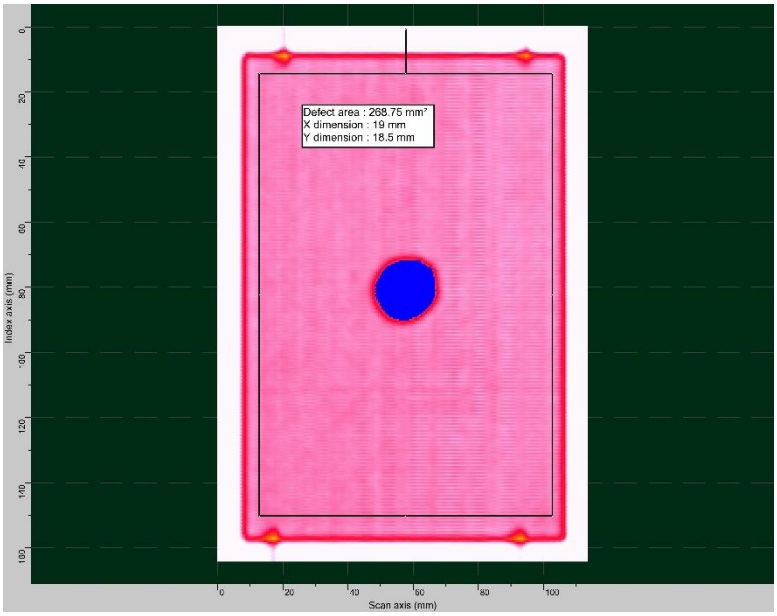


Figure 8 – Through transmission defect analysis of the same specimen as shown in Figure 7 (scanned using 5 MHz 0.5" element size with a 3" focus). The black box indicates the analysis area, and the round blue area in the centre is the defect area.

2.6 Attenuation measurements

As stated in ASTM standard E664 [4], transducers used for quantitative attenuation measurements must not have focused lenses, but use the natural beam shape. The generated ultrasonic beam must be entirely confined within the geometry of the specimen to avoid side-wall echoes or edge-diffraction causing errors in the results. Side-wall echoes and edge-diffraction results in some of the incident energy being reflected in a way that will not be received by the receiving probes, giving a measured attenuation value not indicative of the actual material property. The probes used for the attenuation measurements are summarised in Table 2.

Table 2 – Transducers used for attenuation measurements

Nominal frequency (MHz)	Element diameter (inches)	Focal Length (inches)
1.00	0.50	Natural focus
2.25	0.50	Natural focus
5.00	0.25	Natural focus
10.00	0.25	Natural focus

A schematic diagram of the experimental setup to measure the necessary signals in Equation (3) is given in Figure 9, where both through transmission and pulse echo measurements are required. The four measurements made are the front wall echo, first back-wall echo, transmitted sound, and the water transmission signal with no specimen present, over the same path length.

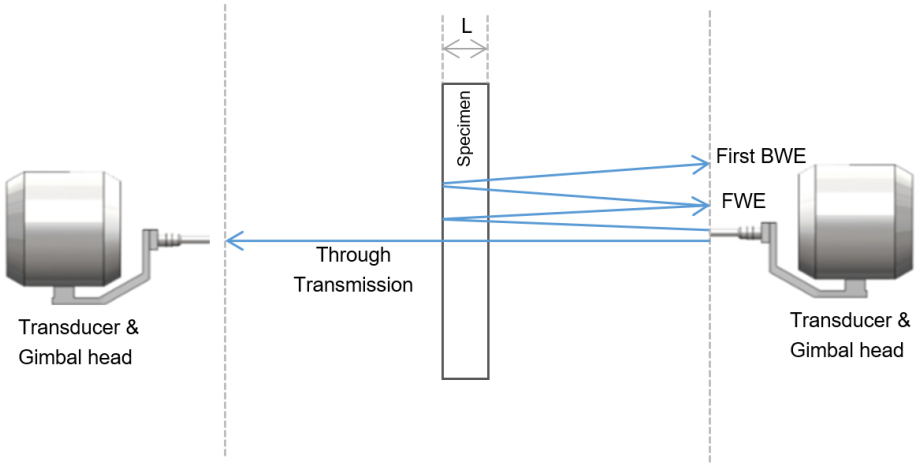


Figure 9 – Experimental setup of the Echo & Transmission Method of measuring acoustic attenuation of a specimen, as described by He [9]. Two transducers are required to measure four signals: the front wall echo, first back wall echo, the sound transmitted through the specimen, and the sound transmitted through water with the same path length.

3. Results

3.1 Defect sizing

Defect size (lateral area in XY) measurements were made using the 6 dB drop method for each case, excluding the 15 MHz probe set. Due to the thickness and material properties, the acoustic attenuation of the carbon-polymer specimens was too high at 15 MHz to discern between areas of damage and pristine areas using the 6 dB drop method, and thus was not included in the analysis. The variation of defect area by transducer frequency is shown in Figure 10. The probe element size and diameter are summarised in Table 1. Note that the 5 MHz transducer used for this comparison has a 0.25” element diameter and a 3” focus.

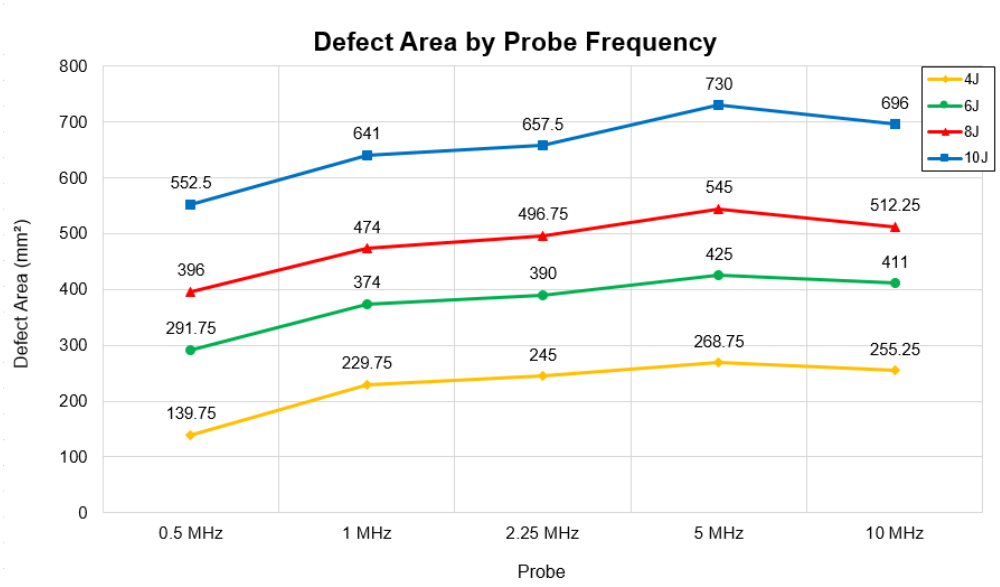


Figure 10 – Effect of transducer frequency on the measurement of defect area. The impact energy is indicated by the colour of the lines.

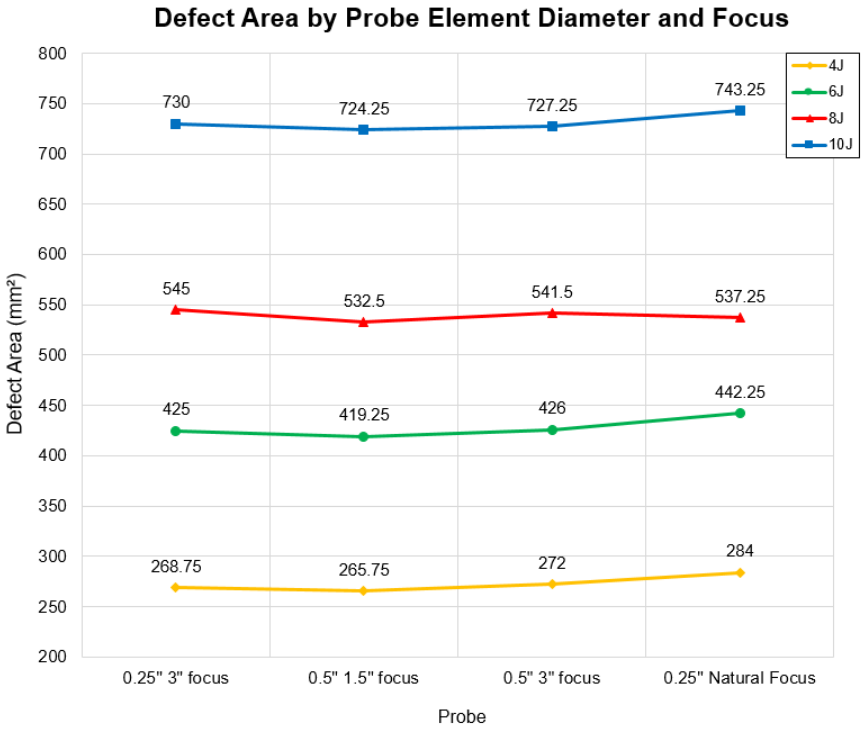


Figure 11 shows a summary of the effect of probe element diameter and focus of a 5 MHz probe on defect sizing.

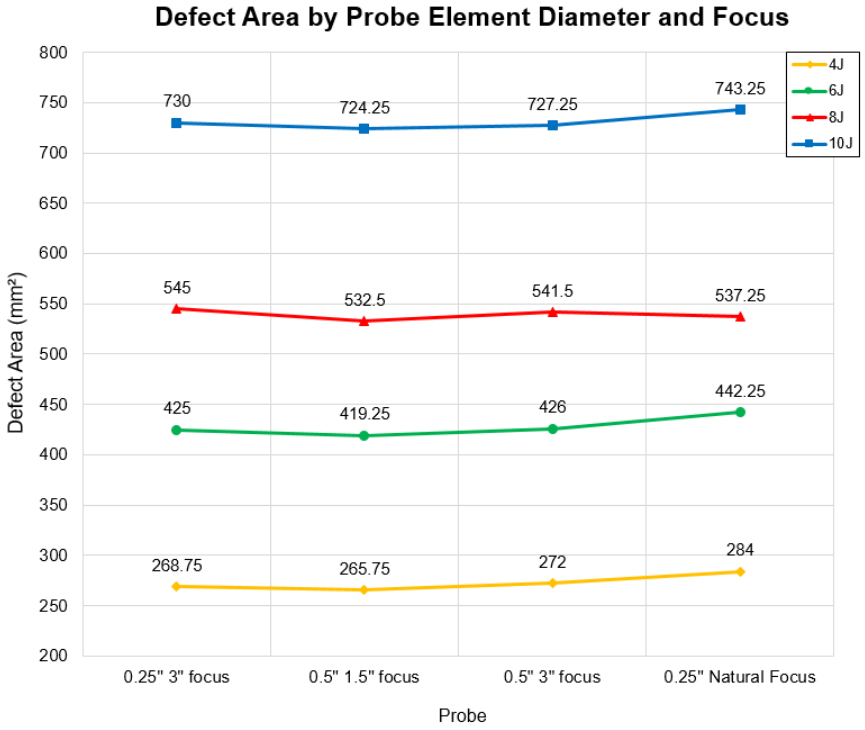


Figure 11 – Effect of element diameter and focal length of a 5 MHz probe on the measurement of defect area.

Using the set of 5 MHz 0.25” element diameter with 3” focus transducers, area measurements were taken on the 6 J impact specimen at the focal length 3”, at 1.5” and at 4.5” away from the specimen. The results are summarised in Figure 12.

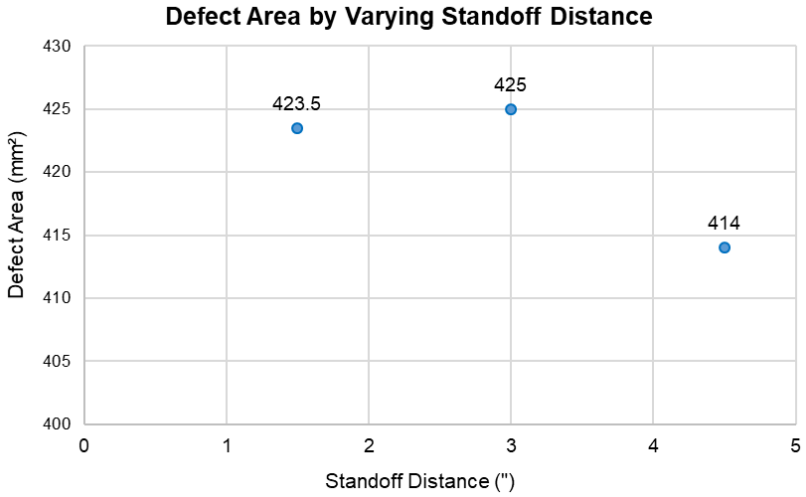


Figure 12 – Defect area by standoff distance of 6 J specimen using 5 MHz probes with 0.25" element diameter and 3" focal length. Note the offset origin.

3.2 Depth analysis

Using the TOF of internal reflections within the 6 J impact sample and the speed of sound of the specimen, the depth at which delaminations occur in the BVID may be measured. For simplicity of comparison between scans using different probes, resulting in different apparent depths, the depths are visualised from 1.5 mm to 4.5 mm with each colour on the colour map representing 0.33mm, Figure 13.

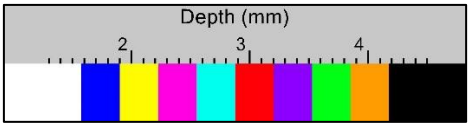
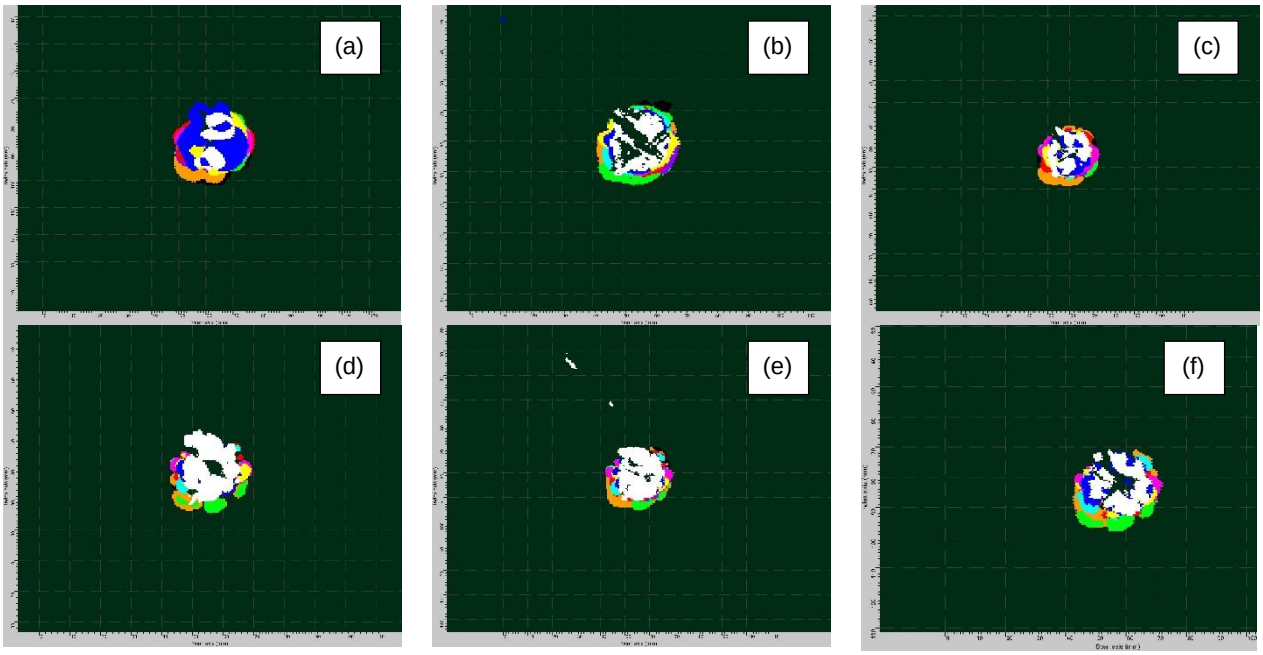


Figure 13 – Defect depth colour map.

Depth analysis was performed using the 2.25 MHz, 10 MHz and 15 MHz transducer sets, as well as all four 5 MHz transducers. The subsequent images are below in Figure 14.



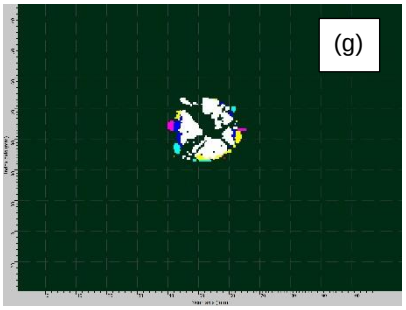


Figure 14 – Depth analysis of 6 J impact sample using (a) 2.25 MHz 0.5” diameter probes, (b) 5 MHz 0.5” element diameter 1.5” focus probes, (c) 5 MHz 0.5” element diameter 3” focus probes, (d) 5 MHz 0.25” element diameter 3” focus probes, (e) 5 MHz 0.25” element diameter naturally focused probes, (f) 10 MHz 0.25” element diameter 1.5” focus probes, and (g) 15 MHz 0.5” element diameter 3” focus probes.

3.3 Attenuation

Acoustic attenuation measurements were taken on the 6 J impact sample in an area of undamaged material, and in both a pristine and repaired section of the repair panel. The four transducers summarised in Table 2 were used for these measurements. The aim of this study was to provide quantitative acoustic determination of the effectiveness of the repair, for subsequent correlation with mechanical post-repair studies, such as compression-after impact. The attenuation curve of the 6 J impact sample is given in Figure 15, showing the increase in attenuation with frequency. The data frequencies in Figure 15 and Figure 16 are lower than the isolated probe centre frequency, especially for probes with a greater centre frequency. This is due to the higher frequency content being filtered by the media due to attenuation.

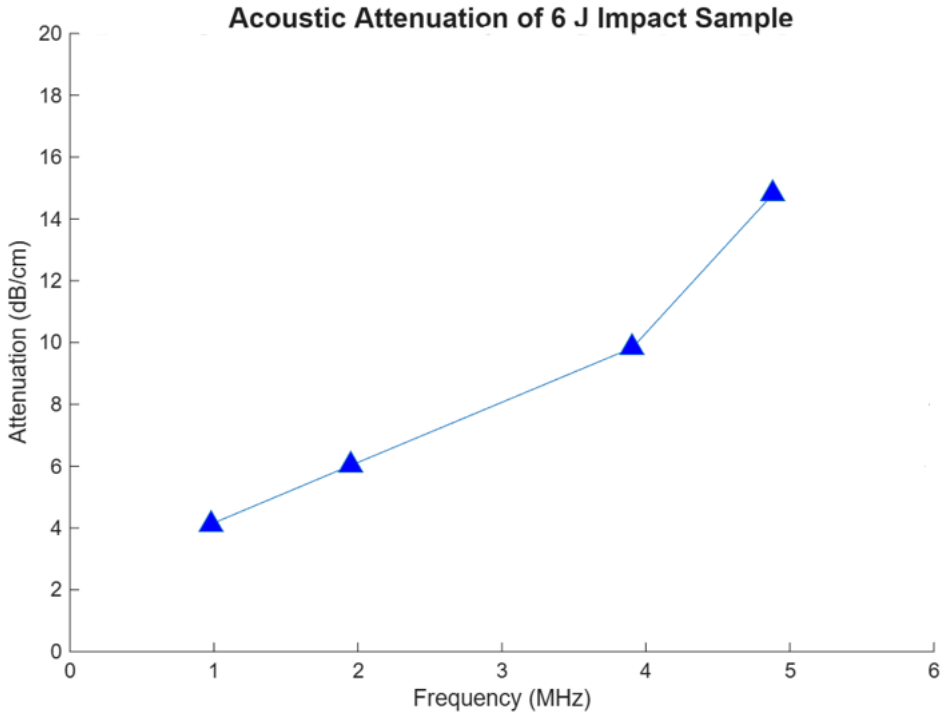


Figure 15 – Attenuation curve of 6 J impact sample

Attenuation measurements were taken at a point in the pristine region of the repaired panel, and at a point in the centre of the repair.

Figure 16 provides the measured attenuation at each point by frequency, demonstrating a clear increase in attenuation over the repair, indicating that this may be a usable method for nondestructive repair quality assessment, if a statistically significant series of post-repair mechanical tests are performed.

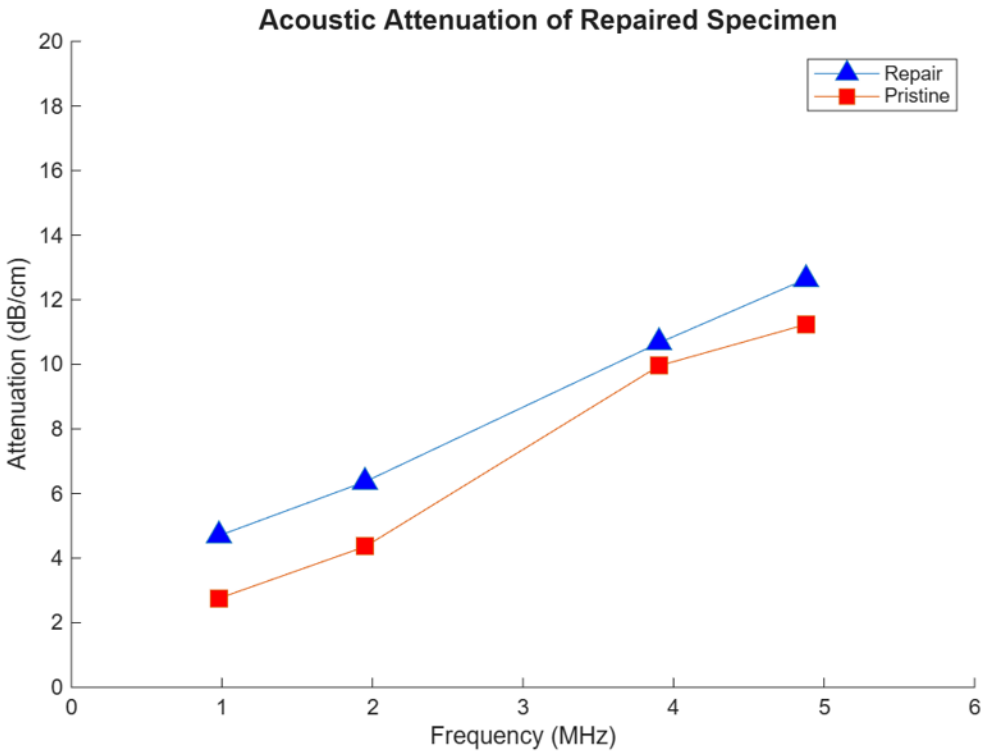


Figure 16 – Attenuation curve of repair panel. A clear increase in attenuation is measurable across the frequency spectrum in the repair.

4. Discussion

By measuring the defect area of the four different energy BVID defects, with probes of six different frequencies, it was found that the apparent defect area varies by 24% for the largest 10 J impact, to 48% for the smallest 4 J impact, quantifying how probe selection can affect ultrasonic measurements. The apparent defect area increases with increasing probe centre frequency, peaking at 5 MHz, and decreasing using 10 MHz transducers. 15 MHz transducers were not suitable for defect sizing due to the higher attenuation at this frequency, and the decrease in defect area using 10 MHz probes from 5 MHz probes indicates that the acoustic attenuation is beginning to affect the defect area sizing past 5 MHz. Defect area measurements using the -6 dB drop method is most accurate using a 5 MHz probe, for this particular material system.

Upon establishing that 5 MHz was the optimum frequency to perform the defect areas sizing, four different combinations of element diameter and focus were used on all four BVID specimens. The variation in defect size across the four probes was between 1.67–6.43%, depending on the impact size. As a smaller element diameter allows for better signal clarity, it was concluded that the 5 MHz 0.25” element diameter with a 3” focus was the most optimal transducer for defect sizing of this material system. Further to this, the effect of the standoff distance on the defect size was also quantified by measuring the defect at 0.5 times the focal length (1.5”) and at 1.5 times the focal length (4.5”). Moving closer into the near field reduced the defect size by 0.35%, and moving away to 1.5 times the focal distance reduced the defect size by 3.59%. This highlights that while taking measurements inside or outside of the focal distance of the probe does not greatly affect the defect sizing using the -6dB drop method, care should be taken to maintain the correct standoff distance for accuracy and repeatability.

Defect depth analysis was undertaken on the 6 J BVID sample. The 0.5 MHz and 1 MHz probes produced wide reflections, making it difficult to isolate the internal reflections from the front wall and back wall reflections, making these frequency probes not suitable for depth analysis. The combining of front wall echo with internal delamination echoes is apparent in the 2.25 MHz defect image, where delaminations occurring between 1.5 mm and 1.88 mm (white) were not visible, most likely due to the end of the front-wall echo pulse occurring at this time, therefore the internal echo gate was not accidently placed at the time in which the internal reflections would occur. The higher attenuation at

15 MHz was apparent in the depth analysis by the loss of internal echoes. Figure 14 (c), (d), (e) and (f) all show similar features at similar depths. It can be inferred that 5 MHz and 10 MHz frequency transducers are most suitable for depth analysis of this carbon-polymer material due to their pulse widths and attenuation response. For further analysis as to at which location delamination occurs, the colour scale can be set for each colour to represent each layer in the layup. This information can be applied to aid repair, or to indicate at which plies delaminations commonly occur due to different types of damage.

Attenuation measurements were taken using sets of 1 MHz, 2.25 MHz, 5 MHz, and 10 MHz transducers. 0.5 MHz probes were not suitable to measure the attenuation of the carbon-polymer materials as the signal width of the pulse-echo reflections was too large resulting in the overlapping of the front wall and back wall echo, making it difficult to separate the two for frequency analysis. Using the 'Echo & Transmission Method' to measure acoustic attenuation gave an expected increase in attenuation proportional to frequency creating an attenuation curve close to linear. As the attenuation is specific to material manufacture and layup, the attenuation curve has a slight variation between the impact sample and the repaired sample. When comparing the measurement made in a pristine region to the repaired region, the attenuation is higher through the repair. This could be caused by more adhesive being used in this area, or small air bubbles in the epoxy.

This method of acoustic attenuation measurement has proved suitable and easily repeatable to complete measurements on repaired carbon-polymer composite panels. This has the potential to be applied to assess the quality of repairs. To further validate this method it is proposed to implement this method whilst completing quality assurance ultrasonic C-Scans of repaired composite materials that are to undergo static or fatigue load testing. The load at which the specimen fails at can then be related to the attenuation of the repair.

5. Conclusion

To conclude, the selection of transducers and system setup for ultrasonic immersion NDT of carbon-polymer composite materials is integral for the accuracy and repeatability of qualitative analysis of material and defect properties. The use of acoustic attenuation as a means to quantitatively, rather than qualitatively, characterise the properties of a repair to a carbon-polymer composite panel has proven possible. Development is expected to further progress the measurement technique and capability to measure acoustic attenuation across multiple points in a repaired specimen.

Further work identified to extend this research and connect to in-field methods of NDT includes using a series of contact phased array transducers to measure the defect sizes of the four impact damages, varying the probe frequency, number of elements and other system parameters. Additionally, quantitative measurement of the effectiveness of the ultrasonic repair assurance measurement by post-repair mechanical testing and correlation would be useful.

6. Acknowledgements

The authors wish to acknowledge the contributions of a number of staff from DSTG in the preparation and completion of this work: Dr Steve Burke, for helpful discussions, Joseph Dominguez in the management of the research area, Pat Frezza and the Multi-Functional Materials Group for the provision of composite test specimens used in the work, and Adam Carpinteri, Structures and Materials Experimentation Group, for the controlled addition of damage to the test specimens.

7. Contact Author Email Address

Contact author email address: hannah.spratling@defence.gov.au

8. Copyright Statement

The authors confirm that they, and/or their company or organization, hold copyright on all of the original material included in this paper. The authors also confirm that they have obtained permission, from the copyright holder of any third party material included in this paper, to publish it as part of their paper. The authors confirm that they give permission, or have obtained permission from the copyright holder of this paper, for the publication and distribution of this paper as part of the ICAS proceedings or as individual off-prints from the proceedings.

References

[1] B. G. Martin. ‘Ultrasonic attenuation due to voids in fibre-reinforced plastics’, *NDT International*, 9 (5), 242-246 (1976).

[2] M. A. Goñi and C.-E. Rousseau. 'On the validity and improvement of the ultrasonic pulse-echo immersion technique to measure real attenuation', *Ultrasonics*, 54 (2), 544 (2014).

[3] J. Blitz and G. Simpson. *Ultrasonic Methods of Non-destructive* Testing (Springer Netherlands, 1995).

[4] American Society for Testing and Materials. ASTM E664, Standard Practice for the measurement of the Apparent Attenuation of Longitudinal Ultrasonic Waves by Immersion Method (ASTM International, 2020).

[5] TecScan Canada. 'Scan3D Systems', https://tecscan.ca/products/ultrasonic-immersion-scanners/scan3d-high-precision-immersion-scanners/.

[6] R.A. Harris, D.H. Follett, M. Halliwell and P.N.T. Wells. ‘Ultimate limits in ultrasonic imaging resolution’, *Ultrasound in Medicine & Biology*, 17 (6), 547-558 (1991).

[7] Iowa State University Center for Nondestructive Evaluation. 'Transducer Types’, https://www.nde-ed.org/NDETechniques/Ultrasonics/EquipmentTrans/transducertypes.xhtml, (2021)

[8] R.A. Smith. ‘Ultrasonic defect sizing in carbon-fibre composites – an initial study’, *INSIGHT – The Journal of the British Institute of NDT*, 36 (8), 595-605, (1994).

[9] P. He and Z. Jun. in *Ultrasonics*; Vol. 39 (Elsevier Science, Amsterdam, 2001), p. 27-32.

[10] Y. Bar-Cohen, A.K. Mal and C.C. Yin. ‘Ultrasonic evaluation of adhesive bonding’, *ASNT Handbook*, 6 (1972).

[11] P. H. Rogers and A. L. Van Buren. 'An exact expression for the Lommel-diffraction correction integral', *Journal of the Acoustical Society of America*, 55 (4), 724 (1974).

[12] P. J. Rae and E. N. Brown. 'Some observations on Measuring Sound Speeds in Polymers Using Time-of-Flight', *Experimental Techniques*, 40 (3), 1085 (2016).

[13] V. A. Del Grosso and C. W. Mader. 'Speed of sound in pure water', *Journal of the Acoustical Society of America*, 52 (5B), 1442 (1972)